Dear Robert McNabb,

Thank you for agreeing to review this manuscript and taking the time to provide general/specific/grammar/typo comments. Your comments certainly helped improve the manuscript and we hope our specific responses adequately address the comments/concerns. Detailed responses for each comment are below; black font is the original comment, blue text is the direct response to the comment, and red text is the updated and/or new text added to the manuscript.

Sincerely,

Dakota Pyles and co-authors

In this manuscript, the authors have presented a phenomenal dataset of Svalbard frontal ablation, covering monthly observations over a ten-year period. The dataset itself represents an impressive combination of different approaches/results into a single coherent dataset, and I have no doubt that it will prove useful for the glaciological community. I have one "major"/general comment about the approach and the work, along with a number of line-specific comments.

general comments

I think that at some point, an explanation of how you (or previous studies) selected the glaciers for this study is needed. You mention at line 142 that you start from the 2019 polygons from Kochtitzky et al. (2022b). I wasn't able to track that file down from the supplemental/data availability given in that paper, but I did find the **Arctic_marine_terminating_fluxgates.gpkg** file (https://github.com/willkochtitzky/FrontalAblation/blob/main/Arctic_marine_terminating_fluxgates.gpkg). From this, I found (I think?) 147 glaciers, based on filtering that dataset by Svalbard and removing fluxgates with "No longer" as a comment. That fits with the "RGI boxes" and "tidewater glacier basins" (line 12) you report, but I'm not sure I understand where the 151 number comes from. It doesn't come from RGI v7.0 (190 glaciers in region 07-01 with term_type = 1), or from RGI v6.0 (134 glaciers in region 07-01 with TermType = 1). Presumably, this is due in part to the RGI outlines often dividing a single terminus into multiple glaciers, combined with removing glaciers that are not marine-terminating over the full study period, but I think this should be stated/explained more clearly - especially if you are then tying this back to the RGI (which version? I can't find this outside of the Fig. 1 caption) with the "RGI-ID".

Looking at the dataset that you have provided, I do see the 2019 polygons, but I am less sure I understand the distinction between the "RGI box"/"glacier basin" and "glacier" as a result. Here, there are some RGI boxes that contain multiple polygons (for example, Nordre Buchananisen). This makes sense given the size of the glaciers included there, but there are also RGI boxes that nearly completely overlap (for example, Nuddbreen and Strongbreen), and I don't understand why these glaciers are not merged as has been done for a number of other RGI glaciers that converge in a single terminus (for example, the Nathorstbreen/Doktorbreen system). Additionally, there are boxes that don't fully encompass the glacier polygon (e.g., Doktorbreen). I think this does need to be clarified/explained in the text, and possibly revised in the dataset itself.

It's a good thought to investigate this and we appreciate the effort looking into Will Kochtitzky's data, but it is not as confusing/inconsistent as it appears to be. Still, we will make the distinction between 151 glaciers and 147 basins clearer in the manuscript text, as well as the RGI version being used.

The 151 glaciers come from an additional GeoJSON file Will shared with us through personal contact, which contained the distinct tidewater glacier termini that he distinguished/digitized in summer 2019 when manually mapping calving front positions for his decadal study (Kochtitzky et al., 2022b). This file was the source of the "2019 polygons". Will included the RGI version 6 ID in this GeoJSON for each of the 151 termini; if there were multiple distinct termini in a single RGI v6 feature, Will defined them as separate features but gave them the same RGIId tag. This explains how there are 151 "glaciers" and only 147 "basins"; four of the 147 basins contain two distinct tidewater glaciers defined by Will (i.e. Nordre Buchananisen as you noticed, also Kongsbreen, Valhallfonna E, and Smeerenburgbreen). As you also found, we included the 2019 polygons that Will digitized as a layer in our GeoPackage, which shows the 151 features. For the four RGI ID's that had two distinct termini, because they had the same RGI ID, we processed both "glaciers" together (i.e. fluxgates/ice discharge, segmentation predictions, CMB correction, etc.), summing quantities or merging geometries as necessary. We handled the processing with great attention to detail, and therefore in the manuscript generally refer to our results/study scope as having 147 (not 151) glaciers.

The previous paragraph answers several of the comments in the second paragraph you wrote, but to clarify the remaining points, the "RGI box" and "glacier basin" are the same thing; the RGI box just refers to the geometry encompassing the basin (used primarily for SAR image sampling), and we chose the word "basin", instead of "glacier", as each studied area/feature was not a single glacier. We do see why it can be confusing as to why we didn't merge the largely overlapping RGI boxes, but this again comes from Will defining those glaciers (i.e. Nuddbreen and Strongbreen) as separate glaciers. The overlapping doesn't matter for downstream tasks because we took care to create very specific postprocessing RGI box geometries that had no overlaps with adjacent glaciers. Will also defined the Nathorstbreen/Doktorbreen system as just one glacier, even though the terminus is fed by 5+ distinct RGI v6 features. Finally, thanks for recognizing that the Doktorbreen RGI box (and maybe other basins) doesn't completely cover the 2019 polygon. We already stated that some of the RGI boxes are manually moved in Sect. 3.1.3, which explains why that RGI box is like that:

While rare, the position of an RGI box may be manually adjusted to facilitate an optimal sampling extent.

To be more clear, while preparing this study we learned that it indeed caused problems for the RGI box to not completely cover the fluxgate geometry, as this creates issues with the CMB polygon area correction; to your point, the RGI box encompassing the 2019 polygon doesn't matter because we only care about the calving front. However, we took particular care to process Doktorbreen correctly, which needed specific attention due to this geometry mistake. Therefore, we are confident the dataset is fine and doesn't need revisions. We updated the manuscript text in the first paragraph in Sect. 3.1.3 to the following:

A critical step for processing frontal area changes is defining a consistent sampling geometry for each Randolph Glacier Inventory version 6 (RGI) basin that contains at least one marine-terminating glacier. To identify all tidewater glaciers in Svalbard, we use the manually digitized termini polygons from summer 2019 in Kochtitzky et al. (2022b), hereafter called the "2019 polygons"; detailed mapping dates can be found at https://doi.org/10.5281/zenodo.19481461. We refer to the sampling geometries as "RGI boxes", which are created by buffering the minimum bounding envelope of all 2019 polygons per RGI-ID by two kilometers, ensuring that the sampling extent captures all frontal changes (i.e. sustained retreat or advance) between 2015-2024. While rare, the position of an RGI box may be manually adjusted to facilitate an optimal sampling extent. In total, 147 RGI boxes are defined, encompassing 151 marine-terminating glaciers (defined by Kochtitzky et al., 2022b), with four RGI boxes containing two separate glaciers. The two distinct 2019 polygons in these four boxes (RGI60-07.00703, RGI60-07.00854, RGI60-07.01354, and RGI60-07.01482) have the same RGI v6 ID, and therefore in downstream tasks are processed together and handled as one RGI basin. Some RGI boxes have large spatial overlaps with adjacent boxes (i.e. glaciers that merge into a single terminus; RGI60-07.00296 and RGI60-07.00422), however, we retain such cases as individual glacier basins, consistent with their definition in Kochtitzky et al. (2022b). In addition to the RGI box vector geometry, a reference raster and geotransform are generated by rasterizing each box onto a 10 m spatial grid in the WGS84 UTM zone 33N coordinate reference system (EPSG:32633), enabling a consistent georeference for downstream raster processing.

minor/specific comments

l. 36, "Arctic": I'm not sure that Yahtse (Bartholomaus et al., 2013) or LeConte (Sutherland et al., 2019) Glaciers can really be characterized as "Arctic" tidewater glaciers. I think this should either be modified (removing "Arctic"), or additional references specific to Arctic glaciers should be included here. Given that most of this paragraph pertains to tidewater glaciers in general, I would drop "Arctic".

Done, we chose to drop “Arctic” in the end.

l. 44, 53: while Table 1 in McNabb et al. (2015) only reports results for the full time period (ca. 1985 - 2013), the calculations are done on much smaller timescales, and plotted as an aggregated annual time series (Fig. 7). The utility of this for modelling is low, especially in comparison to the work presented here, but the results/discussion do at least include the interannual variation/trend for frontal ablation in the region.

Thanks for the clarification on your 2015 study, we just misunderstood how the data were aggregated/presented. We have moved the study to be mentioned in the same context as the annual and seasonal studies of Minowa et al. (2021) and Fahrner et al. (2025). The updated text in that paragraph is now:

Currently, McNabb et al. (2015), Minowa et al. (2021), and Fahrner et al. (2025) are the only regional scale studies that partitioned ice discharge and terminus mass changes at annual or seasonal resolution. However, each study calculated frontal ablation for a select subset of tidewater glaciers across their broader study regions; McNabb et al. (2015) considered 27 Alaskan glaciers with large, active calving fronts and aggregated frontal ablation annually over 1985-2013, Minowa et al. (2021) derived annual estimates for 38 major glaciers in the Patagonia icefields between 2000-2019, and Fahrner et al. (2025) delivered a seasonal (3-monthly) frontal ablation dataset for 49 tidewater glaciers on the Greenland Ice Sheet from 1987-2020.

Fig. 3: I suggest swapping panels a) and b), so that the context map is on the top, labeled a); the large panel showing all of Kongsfjorden could then be labeled b), and the detailed inset of Kronebreen could be labeled c). I also suggest showing the context box for the Kronebreen detail within the larger panel.

Good design suggestions. We weren’t sure of the best way to present the 3 panels (a, b, c), but this is quite helpful. We’ve integrated these changes now into Figure 3 and have reordered/adjusted the figure description, as well as in-text references to the figure’s various panels.

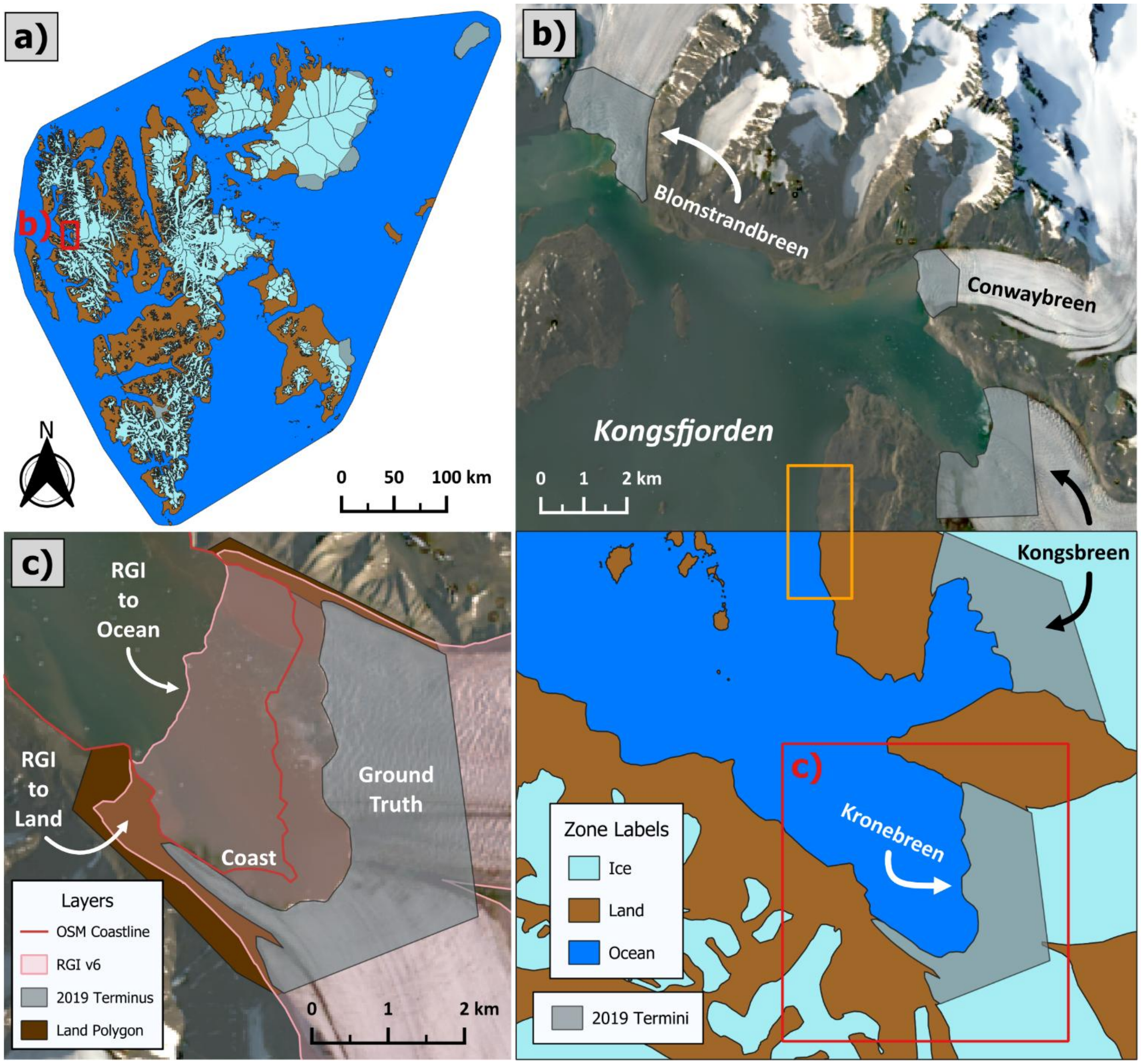

Figure 3. a) Full Svalbard regional extent of the updated ice, ocean, and land zone labels. A red inset map of the zoomed window in (b) focuses on the Kongsfjorden where Kronebreen (panel c) is located. **b)** Spatially contiguous top and bottom subpanels (see land-ocean area within orange box) of the Kongsfjorden and its four tidewater glaciers, showing zone label accuracy with respect to the reference optical image. The top panel shows the termini polygons manually delineated by Kochtitzky et al. (2022b) in 2019, with the Landsat-8 image (July 28, 2019) they used for front mapping plotted as background. Bottom panel is the resulting zone labels at the terminus after applying the layers and processing steps in (c); compare Kronebreen in panels (c) and (b) for a before/after example. **c)** An overview for updating the RGI v6 ice extent at the Kronebreen terminus to the ground truth front position mapped by Kochtitzky et al. (2022b), which results in updated ocean and land zone labels around the glacier outlet area. The OpenStreetMap coastline (© OpenStreetMap contributors, https://www.openstreetmap.org/copyright) provides a reference for maintaining the land-ocean interface during zone label updates, and assists in illustrating the enclosed RGI v6 areas (pink) that become land/ocean. The workflow is applied to all 147 tidewater glacier basins.

l. 221: I think that this assumption is something that you could test using, for example, the rates of advance/retreat reported from previous studies, or from your own results.

We tested the assumption by calculating the ice area variability using our glacier domain polygons for each glacier over the full study period. This variability was computed as the area of the symmetric difference between the largest and smallest observed glacier extents, normalized by the area of the postprocessing RGI box (i.e. only valid ice-ocean area). The postprocessing RGI boxes are already tuned to only include ice bodies that are connected to ocean, making them the ideal geometry for this calculation, compared to the standard RGI box, which includes all zone types and is generally used for SAR image sampling. We found a median ice area variability percentage of 3.9% (95^{th} percentile 17.6%) across all glaciers, with 117 of 147 glaciers having a variability less than 10%.

We also computed the maximum area of disagreement between the static ice mask and either observed glacier extent, normalized by the postprocessing box area for each glacier. This approach provides a conservative upper bound on the impact of using a fixed ice mask for reference-image quality sampling. We found a median static-mask area error of 2.7% (95^{th} percentile 11.6%) across all glaciers, with 134 of 147 glaciers having a mask area error less than 10%.

We adjusted the manuscript text with the following:

While the masks are static and glacier termini evolve throughout the study period, retrospective analysis using the minimum and maximum observed monthly glacier extents (see Sect. 3.1.5) demonstrates that frontal displacement is small relative to glacier outlet area. Across all glaciers, the median maximum disagreement between the static ice mask and the observed glacier extents over the study period is 2.7% (95th percentile: 11.6%) of the outlet area. Similarly, the median glacier area variability between the minimum and maximum observed monthly extents is 3.9% (95th percentile: 17.6%) of the outlet area. These results support the use of static ice and ocean masks as a close approximation of the regions sampled for reference image quality ranking.

l. 222-226: can you provide additional detail about these metrics, or provide references for them? Metrics (2) and (3) seem straightforward enough (assuming that 'median intensity contrast' is just the difference between the median of ice-classed pixels and the median of ocean-classed pixels), but the others are less clear.

We added additional details about the seven metrics used to rank SAR image quality in a new section in the supplement document (Sect S1.1). We also slightly updated the names of some of the seven metrics and put a reference to the new supplement section in the manuscript text:

Seven statistical metrics describing ice-ocean separability and noise characteristics are computed from the sampled backscatter values: (1) a normalized percentile overlap metric, (2) the median intensity contrast, (3) the mean ice-to-ocean intensity ratio, (4) the ice-ocean Shannon entropy difference, (5) the ocean dark-pixel fraction, (6) the ice-to-ocean coefficient of variation ratio, and (7) a Kolmogorov-Smirnov contrast metric (Kolmogorov, 1933). The metrics are standardized and combined using a principal component analysis, with the first component used as a composite image quality score. The composite score is sorted such that higher scores correspond to stronger ice–ocean contrast, and images are ranked accordingly within each RGI-ID per year. Detailed definitions of the individual image quality metrics are provided in the supplementary material (Sect. S1.1).

In the supplement, each metric has a brief description of how it was calculated, accompanied with an equation for clarity.

S1.1 SAR image quality ranking metrics

The reference SAR image ranking is based on seven complementary statistics derived from the sampled ice and ocean backscatter distributions to characterize their separability and additional characteristics associated with SAR image quality. These statistics are standardized and combined using principal component analysis as described in Sect. 3.1.4. For clarity, we provide a brief description and mathematical definition of each statistic.

The normalized percentile overlap metric (O) is computed as the overlap between the 5th–95th percentile intensity ranges of the sampled ice and ocean backscatter distributions, normalized by the combined percentile span of the two distributions,

$$O = \frac{max(0, min(\rho_{ice,95}, \rho_{ocean,95}) - max(\rho_{ice,5}, \rho_{ocean,5})}{max(\rho_{ice,95}, \rho_{ocean,95}) - min(\rho_{ice,5}, \rho_{ocean,5})} \quad (1)$$

where smaller values indicate better separation between the two classes. The median intensity contrast (ΔM) is computed as the difference between the median ice and ocean backscatter,

$$\Delta M = \tilde{I}_{ice} - \tilde{I}_{ocean} \quad (2)$$

where larger values indicate stronger contrast. The mean ice-to-ocean intensity ratio (R) is computed as,

$$R = \frac{\bar{I}_{ice}}{\bar{I}_{ocean}} \quad (3)$$

measuring the relative brightness of glacier ice compared with ocean. The ice-ocean Shannon entropy difference (ΔH) is computed as the difference between the Shannon entropy (Shannon, 1948) of the sampled ice and ocean intensity histograms,

$$\Delta H = H_{ice} - H_{ocean} \quad (4)$$

where larger absolute values indicate greater differences in intensity complexity (texture) between the two classes. The ocean dark-pixel fraction (f_{dark}) is computed as the fraction of sampled ocean pixels with intensities below one-half of the ocean median,

$$f_{dark} = \frac{N(I_{ocean} < 0.5\, \tilde{I}_{ocean})}{N_{ocean}} \quad (5)$$

where larger values indicate a greater proportion of low-backscatter ocean pixels. The ice-to-ocean coefficient of variation ratio (R_{CV}) is computed as the ratio of the coefficients of variation ($CV = \sigma/\mu$) of the sampled ice and ocean intensities,

$$R_{CV} = \frac{CV_{ice}}{CV_{ocean}} \quad (6)$$

providing a relative measure of backscatter variability (including speckle) between the ice and ocean classes. The Kolmogorov-Smirnov (Kolmogorov, 1933) contrast metric (K) is computed by multiplying the two-sample Kolmogorov-Smirnov statistic (D_{KS}) by the median intensity contrast,

$$K = D_{KS}\,\Delta M \quad (7)$$

combining the overall distributional separation of the ice and ocean backscatter with the magnitude of their median intensity contrast.

l. 233-242: I really like this approach, and the explanation.

Thanks! We also thought it was a reasonable approach to handle multiple (daily) front predictions per month.

l. 287: how were these glaciers chosen?

The uncertainty testing subset of glaciers were generally chosen subjectively. However, we wanted the 10 glaciers to be representative of the various types of glaciers found around Svalbard so that our mean region-wide frontal uncertainty is accounting for this representation. Specifically, we considered factors such as front length (large/small), geometry/flow type (fjord/ice cap style), glaciers with a documented surge (Doktorbreen/Nathorstbreen system, Strongbreen), complex frontal geometry (Deltabreen and more), as well as a spatially distributed subset across the Svalbard subregions (i.e. 3 glaciers in SS, 2 each in AF and VF, 1 each in NW, NE, BE). For each of these factors, we tried to select at least one glacier that was representative of the criteria. The actual glacier's that were selected were randomly picked based around the combination of these factors.

The representation of selected uncertainty testing glaciers doesn't necessarily match the quantity of glaciers meeting the criteria in Svalbard, however. For example, the majority (> 50%) of Svalbard's tidewater glaciers are "small" glaciers with "simple" (straight) frontal geometry, which the segmentation model tends to perform better on; only 1-2 of the 10 testing glaciers have these characteristics, opposed to 3-4 testing glaciers with "complex" frontal geometry (which is less common among all of Svalbard's glaciers). Given the common presence of "simple" geometry glaciers, relative to our chosen subset, the mean regional frontal uncertainty of 38.1 meters is most likely conservative.

We added a sentence about this in the manuscript and made a reference to see supplement Sect S1.3 for more details:

Uncertainty in the frontal displacement rate ($\sigma_{\dot{L}}$) is estimated by comparing manually delineated and model-predicted glacier domain polygons from the same month (Fig. 6), across a geographically, geometrically, and behaviorally diverse subset of 10 tidewater glaciers (supplement Table S1). The glaciers were manually selected to be representative of the various types of glaciers found in Svalbard (supplement Sect. S1.3), including factors such as variable calving front length, observed surge behavior, complex and simple frontal geometry, and glacier flow type (fjord or ice cap style).

Fig. 6: it looks like the star for Lilliehøøkbreen is in the wrong place - it should be in the red box shown in the inset

We adjusted the star for Lilliehøøkbreen in Figure 6. Originally, it was intentionally placed above the red box for Lilliehøøkbreen because it looked visually cluttered placing the star inside the box, but we shrunk the star and moved it inside the box. Also, we made some small style updates to the figure suggested by the other reviewer (i.e. only one inset map, north arrow, scalebar, etc.). We also rearranged and slightly updated the figure description as such:

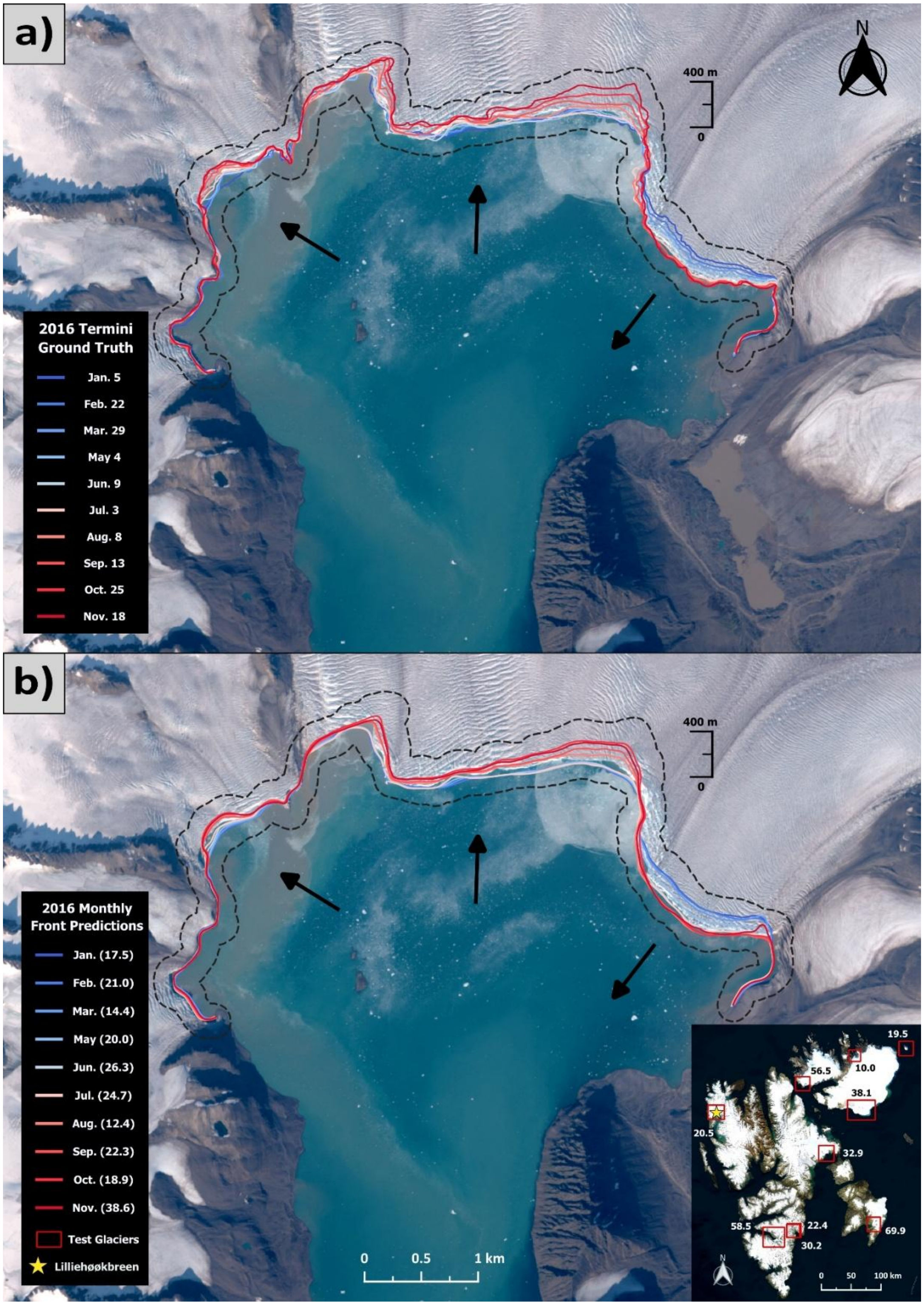

Figure 6. Background for both panels is a Sentinel-2 image obtained on August 2, 2016. **a)** Our 10 manually mapped terminus positions from SAR images at Lilliehøøkbreen glacier over the evaluation period in 2016. Arrows indicate a retreat over the year on the left and middle thirds of the glacier and a frontal advance on the right third. The dashed black line provides a consistent visual reference for

comparing the panels. **b)** The 10 monthly-averaged ice front model predictions, forming pairs with the ground truth positions by the corresponding month. The model captures the observed contrasting retreat/advance pattern during 2016. The width-averaged spatial uncertainty per pair is provided in meters in the legend. The inset map shows the geographic location of all glaciers included in the spatial uncertainty analysis, with the map background given by the Bing Satellite ©. Mean pair spatial uncertainties are annotated in meters on the inset map per testing glacier

l. 391: how many other glaciers had partial elevation change data?

Other than the two island glaciers that we used data from Hugonnet et al. (2021) in the prior sentence/line, there are 11 more glaciers that had partial elevation data. However, this partial data coverage is largely insignificant as 10 of those 11 glaciers were only missing elevation change data at one (8 glaciers) or two (2 glaciers) flux points along their fluxgate geometries. The position of these flux points with missing data tends to be at the edges of the fluxgate and ice extent (i.e. along ice-land boundaries), where the elevation change raster didn't have a valid pixel likely due to radar shadow. The one glacier of the 11 with a larger proportion of partial data (115 of 201 flux points) is Austfonna Basin 5 (RGI60-07.00029) and is due to missing scene coverage. We still chose to use the mean elevation change rate of the 86 available points, as there is adequate spatial coverage to define a reasonable fill value. We updated the manuscript with the following:

We sample ice surface elevation change rates from a $\partial H \partial t^{-1}$ field derived by DEM differencing between 2013-2018 (Malz et al., 2021). Two island glaciers in northeast Svalbard – Kvitøyjøkulen and Storøyjøkulen – are missing surface elevation change data, which is filled with a glacier-specific constant rate from the period January 2015 – 2020 for all flux points (Hugonnet et al., 2021). There are 11 additional glaciers with partial elevation change data due to radar shadow, whose missing flux points are filled with the mean rate of available point measurements. Ten of these glaciers are only missing data at one or two flux points, with the final glacier of the subset missing a larger proportion of points because of poor scene coverage in the DEM differencing.

l. 505-506: as with the comment at l. 221, I think this is something that can be checked/quantified - how big are the changes (as a fraction of the domain area) for all months, for each glacier?

We tested this assumption by comparing the glacier domain polygons immediately before and after each interpolation gap. The area of the symmetric difference between the two polygons was normalized by the mean area of the pre- and post-gap glacier domains, providing a measure of the relative change in the CMB integration domain across each gap. Across 676 interpolation gaps, the median relative domain change was 2.8% (95th percentile: 10.1%). These results indicate that the glacier domain over which CMB was integrated remained highly consistent throughout the interpolation intervals, supporting the use of the first post-gap glacier domain for integrating monthly CMB fields. We revised the manuscript text to include some quantitative reasoning and to sharpen/update the existing text:

While frontal variations are not considered within the gap period, area changes are generally small relative to the glacier domain; across all interpolation gaps, the median relative change between the pre- and post-gap glacier domains was 2.8%, while the 95th percentile was 10.1%. This supports the use of a common glacier domain during interpolation, allowing monthly CMB variability to be retained, rather than restricting CMB sampling to months with available frontal geometry.

l. 510: can you also report the number of months (out of the 15,500) are gap-filled in this way, and how many glaciers have gapless records?

To be clear, the 15,500 months are not the interpolated record, that number is the amount of frontal ablation estimates we have directly computed from consecutive monthly frontal geometries. The total number of frontal ablation estimates, including non-interpolated and interpolated measurements, is 17,340. We have already reported the number of months that are gap-filled in Results section 4.1 (the section immediately after this Line 510, 3.4 section where we are describing the frontal information interpolation). This is the text that was already written in the first two sentences of section 4.1:

In total, of 17,493 possible monthly measurements across the 147 marine terminating glaciers defined in the study, we generate 15,500 estimates of frontal ablation, frontal area change, ice discharge, and CMB constrained to model-predicted frontal geometry from 2015-2024 (88% temporal coverage). An additional 1,840 monthly estimates are produced by linearly interpolating temporal gaps of frontal area change within each glacier's time series, resulting in 99% total temporal coverage (see Sect. 3.4).

Nevertheless, with the new text from your previous comment about Line 505-506, we now have the number of interpolated months reported in this section/paragraph. Unfortunately, none of the glaciers have a gapless record (i.e. 119 monthly frontal ablation measurements) because the postprocessing filters (supplement Sect S1.2) and the manual frontal geometry check/filtering described in Sect. 3.1.5. were quite rigorous (1,057 of 16,704 monthly fronts manually deleted). However, as you suggested, we also added in section 3.4 the number of glaciers that have non-interpolated monthly frontal ablation records of greater than 80, 90 and 95% temporal coverage, as well as information on the total number of monthly frontal ablation measurements (including non-interpolated and interpolated months) and the worst temporally covered glacier. Including the new text from the previous comment in the same paragraph, this is the final updated text in the manuscript:

While frontal variations are not considered within the gap period, area changes are generally small relative to the glacier domain; across all interpolation gaps, the median relative change between the pre- and post-gap glacier domains was 2.8%, while the 95th percentile was 10.1%. This supports the use of a common glacier domain during interpolation, allowing monthly CMB variability to be retained, rather than restricting CMB sampling to months with available frontal geometry. Similarly, as the complete monthly ice discharge time series is independent from frontal geometry, the standard mean discharge is taken over all gap months (see Sect. 3.2.4). With the complete monthly record of ice discharge and CMB, as well as the temporally interpolated frontal area change, the frontal ablation time series is completed with 17,340 monthly measurements. As such, the only temporal gaps remaining are for glaciers whose frontal geometry record begins after January 2015 or ends before December 2024, as we cannot extrapolate frontal information. Although none of the glaciers have a gapless frontal geometry record (i.e. all have interpolated gaps) due to the filtered outliers (see Sect 3.1.5 and supplement Sect. S1.2), 37, 99, and 129 of the 147 glaciers have a non-interpolated monthly frontal ablation temporal coverage of 95, 90, and 80%, respectively. Further, the glacier with the worst non-interpolated temporal coverage is the Doktorbreen/Nathorstbreen system (RGI60-07.01474), with 57 of 119 possible months (~48%).

Table 1 + in-text values: I think you should specify in the table caption that the reported decadal mean uncertainty values are the standard error of the mean uncertainty (i.e., mean(uncertainty) / sqrt(count)). That said, I think the better/more appropriate way to do this would be to calculate the root mean square of the uncertainties, which would give, e.g., -21.57 ± 3.06 for the frontal ablation, -5.60 ± 2.98 for the area change, 17.75 ± 0.65 for the ice discharge, and -1.78 ± 0.28 for the CMB.

We appreciate the suggestion and also think it's a reasonable approach to compute the decadal uncertainty. However, the uncertainty reported for the decadal mean is intended to represent the propagated uncertainty of the arithmetic mean of the independent annual estimates. Accordingly, annual uncertainties are propagated following standard error propagation, yielding $\sigma_{\text{dec}} = \sqrt{\sum_i \sigma_i^2} / N$ (Eq. 20c). The proposed root-mean-square uncertainty, $\sqrt{\sum_i \sigma_i^2 / N}$, instead represents the characteristic uncertainty of an individual annual estimate rather than the propagated uncertainty of the decadal mean. Our intention was to quantify the uncertainty associated with the decadal mean itself by treating the annual estimates as independent measurements with associated uncertainties. To avoid ambiguity, we have clarified this interpretation in the manuscript after introducing equation 20c in Sect. 3.4, before any of the results tables in Sect. 4.1:

The resulting uncertainty represents the propagated measurement uncertainty of the decadal mean and therefore decreases as independent annual estimates are averaged (see Sect. 4.1, Table 1).

Table 2: As for Table 1 - I think the more appropriate way to calculate the decadal uncertainty is as the RMS of the annual uncertainty, rather than the standard error.

Since we defended keeping the decadal uncertainty as currently computed we did not adjust the values in Table 2 or Table 3.

l. 605: how is this intensity index derived? Is it just the frontal ablation normalized by the terminus length (in 100s of km)?

We adjusted the manuscript text to clearly define the frontal ablation intensity and updated the grammar for consistency/clarity:

The final subregion, Vestfonna ice cap (VF), has the lowest decadal rate (-1.03 ± 0.10 Gt a-1) of all regions. However, to facilitate comparisons among regions with different total calving front lengths, frontal ablation is also normalized by the total terminus length and expressed per 100 km of calving front (Table 2). VF has the second highest frontal ablation intensity rate (-2.34 Gt a-1 (100 km)-1) of all regions, revealing the region's relevance for studying controls on and impacts of frontal ablation in Svalbard. Expectedly, AF exhibits the strongest frontal ablation intensity (-4.19 Gt a-1 (100 km)-1), further demonstrating its dominant contribution to Svalbard's frontal ablation mass budget.

l. 609: similar to the intensity index, would it make more sense to compare the CMB correction normalized by the area between the flux gate and the terminus, rather than the magnitude?

Yes, this makes sense, and we opted to report both the absolute CMB magnitude and the specific CMB in the revised manuscript. The specific CMB was calculated by normalizing the regional CMB by the mean glacierized area of each region, where the regional glacierized area was computed by summing the mean annual glacier domain areas of all glaciers within each region. The revised text now reads:

Although the largest absolute CMB correction occurs in AF (−0.48 ± 0.03 Gt a^{-1}) and SS (−0.56 ± 0.03 Gt a^{-1}), the specific CMB (Table 2) is most negative in SS (−1.86 m w.e. a^{-1}), NW (−1.60 m w.e. a^{-1}), and BE (−1.06 m w.e. a^{-1}), indicating that these regions experience the strongest climatic mass losses relative to their glacierized area.

Table 2. Decadal frontal ablation, frontal area change, ice discharge, and CMB rates for the seven glaciated subregions of Svalbard. Monthly coverage is calculated as the percent of available measurements from total possible months, based on the number of glaciers in the region. Peak year indicates when the region's frontal ablation mass loss was most negative between 2015 and 2024. Termini

length is the decadally-averaged, summed length of all glacier fronts corresponding to the region. FA per 100 km is the region's decadal frontal ablation rate normalized per 100 km of terminus length. Specific CMB is the region's decadal CMB rate normalized by the mean glacier domain area of the region.

	Decadal Regional Total Rates (Gt a^{-1})				Statistics				
Region	Frontal Ablation	Frontal Area Change	Ice Discharge	CMB	Monthly Coverage (%)	Peak Year	Termini Length (km)	FA per 100 km (Gt a^{-1})	Specific CMB (m w.e. a^{-1})
AF	-10.38 ± 0.63	-2.12 ± 0.62	8.74 ± 0.13	-0.48 ± 0.03	89	2015	248	-4.19	-0.53
BE	-1.42 ± 0.29	-0.73 ± 0.28	0.96 ± 0.05	-0.26 ± 0.01	66	2021	73	-1.96	-1.06
KV	-1.86 ± 0.61	-0.72 ± 0.60	1.17 ± 0.11	-0.04 ± 0.00	95	2018	101	-1.83	-0.44
NE	-2.55 ± 0.15	-0.73 ± 0.15	2.01 ± 0.04	-0.18 ± 0.01	90	2016	131	-1.94	-1.02
NW	-1.75 ± 0.13	-0.38 ± 0.11	1.59 ± 0.07	-0.21 ± 0.01	89	2016	116	-1.53	-1.60
SS	-2.58 ± 0.14	-0.70 ± 0.13	2.44 ± 0.04	-0.56 ± 0.03	87	2023	145	-1.77	-1.86
VF	-1.03 ± 0.10	-0.22 ± 0.10	0.85 ± 0.03	-0.04 ± 0.00	89	2016	44	-2.34	-0.63

l. 634, elsewhere: "Negribreen" is "Negri Glacier", so you can remove "glacier" after Negribreen (and any glacier name that includes "breen")

Good to know. This was a common mistake throughout the manuscript; all cases have been fixed.

Table 3: as for Table 1

See author comment for the Table 1 + in-text values comment.

Section 5.1: I wonder if a portion of the difference between your results and Kochtitzky et al. (2022b) is due to the difference in ice thickness datasets used - either by spatially distributing observations from GlaThiDa, or from filling in with Millan et al (2022)'s results - compared to the SVIFT results (Fürst et al., 2018a) used here. How large are the differences for the thicknesses at your fluxgates compared to the results in Kochtitzky et al., for example? Could you plot, as a supplemental figure, the ice thickness along the flux gate used for both studies, at least for 1-2 glaciers with large differences?

We compared the mean ice thickness between this study and Kochtitzky et al. (2022b) for each glacier, as well as the correlation between ice thickness differences and frontal ablation differences (supplement Fig. S5, below). We also plotted the pointwise mean ice thickness in this study (100 m resolution) across the fluxgate and that of Kochtitzky et al. (25 m resolution); this was done for Austfonna Basin 3 and Perseibreen, which have the largest frontal ablation difference and mean ice thickness difference between the studies, respectively. We updated the manuscript text by continuing the glacier-scale comparison paragraph with the following:

In addition, we assessed whether differences in ice thickness reconstruction methods could contribute to the glacier-scale differences in frontal ablation estimates. This study derives ice thicknesses (Sect. 3.2.2) from the SVIFT thickness dataset (Fürst et al., 2018a), whereas Kochtitzky et al. (2022b) primarily used spatially distributed GlaThiDa observations supplemented by Millan et al. (2022) modeled thickness estimates where observations were unavailable. Comparison of mean ice thicknesses at the fluxgates shows a mean absolute difference of 37.7 m (RMSE = 47.3 m) across the 147 glaciers (see supplement Fig. S5). However, absolute thickness differences are not significantly correlated with absolute frontal ablation differences (Pearson $r = -0.08$, $p = 0.31$), suggesting that differences between the thickness datasets are unlikely to be the dominant explanation for the glacier-scale differences in frontal ablation estimates.

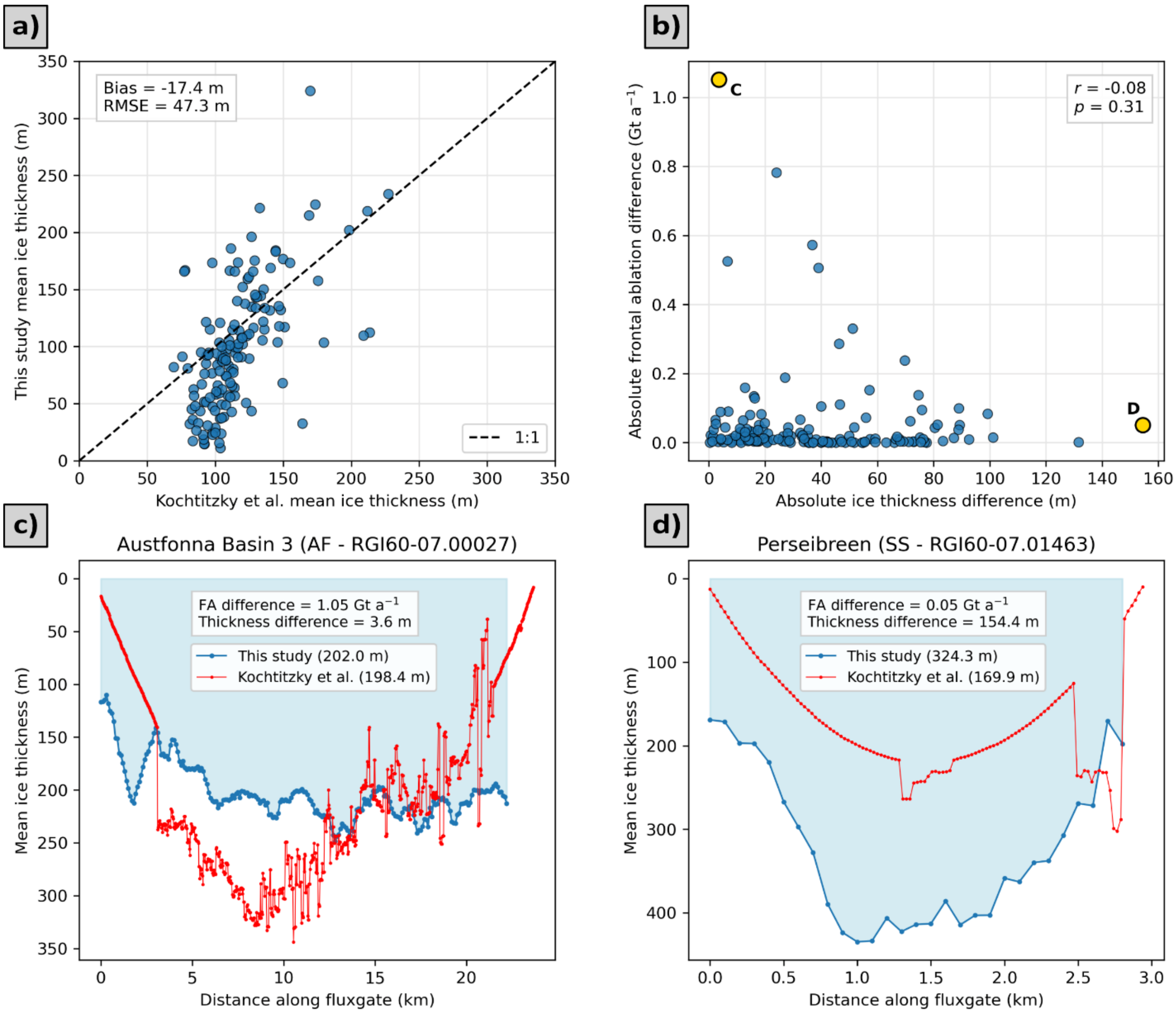

Figure S5. a) Comparison of the mean ice thickness reported by Kochtitzky et al. (2022b) and this study for all 147 tidewater glaciers. On average, our thickness estimates are 17.4 m thinner than those of Kochtitzky et al, with an RMSE of 47.3 m. The dashed line indicates a 1:1 relationship. **b)** Absolute difference in mean ice thickness versus the absolute difference in long-term frontal ablation rate between the two studies. No significant relationship is observed (Pearson r = -0.08, p = 0.31). Yellow points correspond to the example glaciers shown in panels (c) and (d). **c)** Mean ice thickness profile along the Austfonna Basin 3 fluxgate, which has the largest frontal ablation difference between the two studies. Fluxgates are at different spatial positions. **d)** Mean ice thickness profile along Perseibreen fluxgate, which has the largest mean ice thickness difference between the two studies. Fluxgates are at different spatial positions.